J|A|C|S
ARTICLES

Published on Web 02/03/2009

Efficient Kinetic Macrocyclization

Wen Feng,[†] Kazuhiro Yamato,[‡] Liuqing Yang,[†] Joseph S. Ferguson,[‡] Lijian Zhong,[†] Shuliang Zou,[†] Lihua Yuan,*[,†] Xiao Cheng Zeng,*[,§] and Bing Gong*[,‡]

College of Chemistry, Key Laboratory for Radiation Physics and Technology of Ministry of Education, and Institute of Nuclear Science and Technology, Sichuan University, Chengdu, 610064, Sichuan, China, Department of Chemistry, The State University of New York at Buffalo, Buffalo, New York 14260, and Department of Chemistry, University of Nebraska−Lincoln, Lincoln, Nebraska 68588

Received October 7, 2008; E-mail: bgong@chem.buffalo.edu; lhyuan@scu.edu.cn; xczeng@phase2.unl.edu

Abstract: In this article, the highly efficient formation of a series of recently discovered aromatic oligoamide macrocycles consisting of six meta-linked residues is first discussed. The macrocycles, with their backbones rigidified by three-center hydrogen bonds, were found to form in high yields that deviate dramatically from the theoretically allowed value obtained from kinetic simulation of a typical kinetically controlled macrocyclization reaction. The folding of the uncyclized six-residue oligomeric precursors, which belong to a class of backbone-rigidified oligoamides that have been demonstrated by us to adopt well-defined crescent conformations, plays a critical role in the observed high efficiency. Out of two possible mechanisms, one is consistent with experimental results obtained from the coupling of crescent oligoamides of different lengths, which suggests a remote steric effect that discourages the formation of oligomers having lengths longer than the backbone of the six-residue precursors. The suggested mechanism is supported by the efficient formation of very large aromatic oligoamide macrocycles consisting of alternating meta- and para-linked residues. These large macrocycles, having H-bond-rigidified backbones and large internal lumens, are formed in high (>80%) yields on the basis of one-step, multicomponent macrocyclization reactions. The condensation of monomeric meta-diamines and a para-diacid chloride leads to the efficient formation of macrocycles with 14, 16, and 18 residues, corresponding to 70-, 80-, and 90-membered rings that contain internal cavities of 2.2, 2.5, and 2.9 nm across. In addition, the condensation between trimeric or pentameric diamines and a monomeric diacid chloride had resulted in the selective formation of single macrocyclic products with 16 or 18 residues. The efficient formation of the macrocycles, along with the absence of other noncyclic oligomeric and polymeric byproducts, is in sharp contrast to the poor yields associated with most kinetically controlled macrocyclization reactions. This system represents a rare example of highly efficient kinetic macrocyclization reactions involving large numbers of reacting units, which provides very large, shape-persistent macrocycles.

Introduction

Large macrocyclic structures have unique physical properties, special structural features, and chemical behavior that differ from their smaller counterparts.[1] In particular, macrocycles with a persistent shape have attracted wide attention due to their defined structures and potential applications.[2] For example, shape-persistent macrocycles may serve as reliable scaffolds for designing endoreceptors by presenting various convergent functional groups.[4,5] Their well-defined cavities may serve as catalytic sites.[6] Aligning rigid macrocycles into columnar assemblies should lead to robust organic nanotubes.[7] Unfortunately, the formation of large macrocycles is impeded by the entropically disfavored nature of the cyclization process. Due to the large number of monomeric units and the overall flexibility of noncyclic oligomeric precursors, large macrocycles are particularly difficult to synthesize, which is often complicated by low yields and undesired side products.[2] As a result,

[†] Sichuan University.
[‡] The State University of New York at Buffalo.
[§] University of Nebraska−Lincoln.

(1) (a) Meng, Q.; Hesse, M. *Top. Curr. Chem.* **1992**, *161*, 107. (b) Sessler, J.; Burrell, A. *Top. Curr. Chem.* **1992**, *161*, 177. (c) Bernhardt, P. V.; Moore, E. G. *Aust. J. Chem.* **2003**, *56*, 239.
(2) (a) Grave, C.; Schlüter, A. D. *Eur. J. Org. Chem.* **2002**, 3075. (b) Höger, S. *Chem. Eur. J.* **2004**, *10*, 1320. (c) Zhang, W.; Moore, J. S. *Angew. Chem., Int. Ed.* **2006**, *45*, 4416.
(3) Some recent examples of other macrocycles:(a) Xing, L. Y.; Ziener, U.; Sutherland, T. C.; Cuccia, L. A. *Chem. Commun.* **2005**, 5751. (b) Rotger, C.; Pina, M. N.; Vega, M.; Ballester, P.; Deya, P. M.; Costa, A. *Angew. Chem., Int. Ed.* **2006**, *45*, 6844. (c) Sakamoto, J.; Schluter, A. D. *Eur. J. Org. Chem.* **2007**, 2700. (d) Campbell, F.; Plante, J.; Carruthers, C.; Hardie, M. J.; Prior, T. J.; Wilson, A. J. *Chem. Commun.* **2007**, 2240. (e) Zhu, Y. Y.; Li, C.; Li, G. Y.; Jiang, X. K.; Li, Z. T. *J. Org. Chem.* **2008**, *73*, 1745. (f) Alfonso, I.; Bolte, M.; Bru, M.; Burguete, M. I.; Luis, S. V.; Rubio, J. *J. Am. Chem. Soc.* **2008**, *130*, 6137.
(4) (a) Lehn, J.-M. *Supramolecular Chemistry: Concepts and Perspectives*; VCH: Weinheim, 1995. (b) Seel, C.; Vögtle, F. *Angew. Chem., Int. Ed. Engl.* **1992**, *31*, 528.
(5) Rebek, J. *Science* **1987**, *235*, 1478.
(6) Höger, S.; Meckenstock, A.-D. *Chem. Eur. J.* **1999**, *5*, 1686.
(7) (a) Shetty, A. S.; Zhang, J.; Moore, J. S. *J. Am. Chem. Soc.* **1996**, *118*, 1019. (b) Seo, S. H.; Jones, T. V.; Seyler, H.; Peters, J. O.; Kim, T. H.; Chang, J. Y.; Tew, G. N. *J. Am. Chem. Soc.* **2006**, *128*, 9264. (c) Pasini, D.; Ricci, M. *Curr. Org. Syn.* **2007**, *4*, 59.

Scheme 1

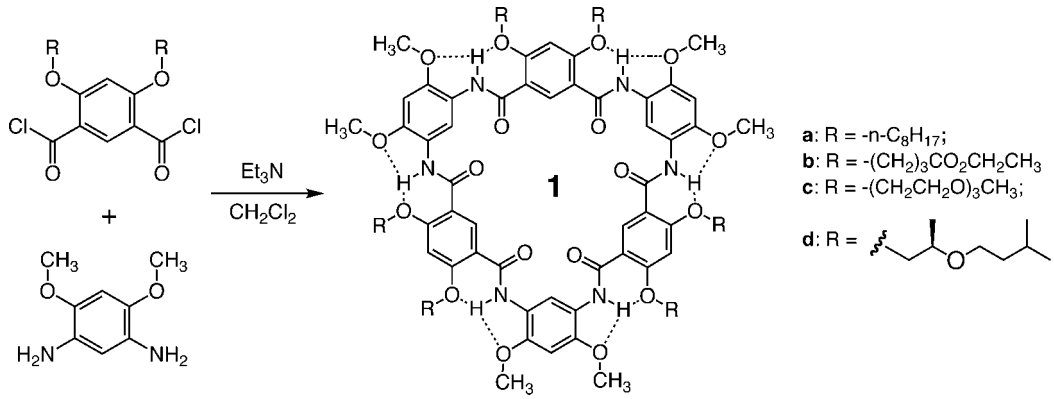

only a few systems of shape-persistent macrocycles are known, the majority of which are those with hydrocarbon backbones formed by stepwise coupling between sp- or sp^2-hybridized carbon atoms.[2,3] To improve the efficiency of macrocyclization reactions, various strategies such as templation,[8] intramolecular ring closure,[9] and reversible (dynamic) covalent bond formation[10] have been adopted.

We recently discovered the highly efficient (>80%) formation of oligoamide macrocycles **1** from the one-step condensation of monomeric diamines and diacid chlorides (Scheme 1).[11] In addition to the ones already reported, analogous six-residue macrocycles with a wide variety of side chains of dramatically different properties have now been prepared in high yields, which demonstrated that the high efficiency of the macrocyclization reaction was independent of the side chains (i.e., R groups). Thus, the formation of the macrocycles was determined by the backbone of these cyclic oligoamides, the noncyclic analogs of which were shown by us to fold into rigid, crescent shapes enforced by intramolecular three-center hydrogen bonds.[12]

This one-step, highly efficient macrocyclization has raised additional questions that need to be addressed. For example, one of the biggest drawbacks of kinetic macrocyclization is that the irreversible nature of kinetically controlled bond formation invariably leads to "overshooting" oligomers that are too long to form the desired macrocycle.[2a] As a result, macrocyclization reactions involving kinetic bond formation are usually complicated by the generation of many byproducts, which significantly lowers the yield of the desired product. How were overshooting products avoided in the formation of macrocycles **1**, which involves kinetically controlled amide-bond formation? Are the observed high yields a phenomenon unique to six-residue macrocycles **1**, or would the same high efficiency be observed for the formation of larger macrocycles with similar aromatic oligoamide backbones?

In this article, we first try to explain the observed high efficiency in the one-step formation of macrocycles **1**. Out of two possible mechanisms, only one is consistent with our experimental results. Such a mechanism involves a remote steric effect resulting from the folded conformations of the reactants, the reacting intermediates, and presumably, the transition state, which impedes the formation of oligomeric precursors with lengths beyond a "cyclizable" range. This mechanism should be of general applicability to kinetic macrocyclization reactions involving oligomeric precursors that fold into rigid, curved conformations. Such a prediction was subsequently confirmed by the formation of large oligoamide macrocycles with backbones consisting of alternating meta/para-linked benzene residues. These large macrocycles were obtained with high overall yields similar to those observed for the smaller macrocycles **1**. The one-step condensation of monomeric reactants led to a product containing three macrocycles with 14, 16, and 18 residues. On the basis of the condensation between trimeric or pentameric diamines and monomeric diacid chloride, single macrocyclic products with 16 or 18 residues were also selectively formed in high yields. Compared to the six-residue macrocycles **1**, these meta/para-linked macrocycles are much larger, with 70-, 80-, and 90-membered rings that contain well-defined, noncollapsible internal cavities of 2.2, 2.5, and 2.9 nm across.

Results and Discussion

Mechanism. It seems that the folding of the uncyclized oligomeric precursors of macrocycles **1** into a crescent conformation, which was demonstrated by us to be enforced by highly favorable intramolecular three-center H-bonds,[12] plays an important role for the efficient macrocyclization. By bringing their two termini into reacting distance upon folding, the precursor of a macrocycle, with its folded, crescent shape, is predisposed for highly favorable intramolecular cyclization. On the other hand, the same shape persistency prevents the ends of shorter or longer oligomers from being brought into close proximity, which retards or prohibits cyclization. In the case of macrocycles **1**, only the oligomeric precursors with six residues have the proper length to cyclize efficiently.

However, a folding-assisted intramolecular cyclization alone cannot explain the observed high overall yields of **1**. While the

(8) McCallien, D. W. J.; Sanders, J. K. M. *J. Am. Chem. Soc.* **1995**, *117*, 6611.
(9) (a) Zhang, J.; Pesak, D. J.; Kudwick, J. L.; Moore, J. S. *J. Am. Chem. Soc.* **1994**, *116*, 4227. (b) Hensel, V.; Lützow, K.; Jakob, J.; Gessler, K.; Saenger, W.; Schlüter, A.-D. *Angew. Chem., Int. Ed. Engl.* **1997**, *36*, 2654. (c) Tobe, Y.; Utsumi, N.; Nagano, A.; Naemura, K. *Angew. Chem., Int. Ed.* **1998**, *37*, 1285.
(10) (a) Gallant, A. J.; MacLachlan, M. J. *Angew. Chem., Int. Ed.* **2003**, *42*, 5307. (b) Gallant, A. J.; Hui, J. K.-H.; Zahariev, F. E.; Wang, Y. A.; MacLachlan, M. J. *J. Org. Chem.* **2005**, *70*, 7936. (c) Zhang, W.; Moore, J. S. *J. Am. Chem. Soc.* **2006**, *127*, 11863.
(11) (a) Yuan, L. H.; Feng, W.; Yamato, K.; Sanford, A. R.; Xu, D. G.; Guo, H.; Gong, B. *J. Am. Chem. Soc.* **2004**, *126*, 11120. (b) Sanford, A. R.; Yuan, L. H.; Feng, W.; Yamato, K.; Flowers, R. A.; Gong, B. *Chem. Commun.* **2005**, 4720.
(12) (a) Zhu, J.; Parra, R. D.; Zeng, H.; Skrzypczak-Jankun, E.; Zeng, X. C.; Gong, B. *J. Am. Chem. Soc.* **2000**, *122*, 4219. (b) Parra, R. D.; Zeng, H. Q.; Zhu, J.; Zheng, C.; Zeng, X. C.; Gong, B. *Chem. Eur. J.* **2001**, *7*, 4352. (c) Yuan, L. H.; Zeng, H. Q.; Yamato, K.; Sanford, A. R.; Feng, W.; Atreya, H. S.; Sukumaran, D. K.; Szyperski, T.; Gong, B. *J. Am. Chem. Soc.* **2004**, *126*, 16528.

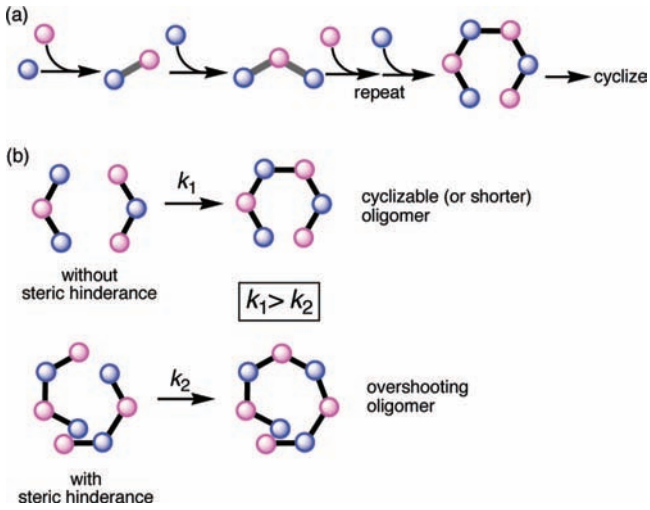

Figure 1. Two possible mechanisms explaining the preferable formation of the immediate precursor of macrocycles **1**. (a) A chain-growth process involving the addition of one monomer at a time until the length of the oligomeric precursor is reached, which requires reaction steps between monomers, or between monomers and oligomers, to be faster than those between oligomers. (b) The absence of steric hindrance in the formation of oligomers with lengths equivalent to or shorter than that of the hexameric precursor. In the formation of oligomers longer than the hexameric precursor, steric hindrance will result due to the crowding of the two remote ends, which retards the reaction (i.e., $k_1 > k_2$).

likelihood of obtaining a given macrocycle depends on the ability of the oligomeric precursor to cyclize, the generation of the macrocycle also depends on the formation of the very precursor. The yields of crude, but nearly pure macrocycles **1** after simple washing, ranged from 85% to 90% (70% to 80% after extensive purification), which deviate dramatically from the theoretically allowed maximum yield (36%) obtained from kinetic simulation.[2a]

The efficient formation of macrocycles **1** and the dearth of other longer oligomers necessitate the cyclizable six-residue oligomers to form preferably in the chain-extension process. Two mechanisms satisfying such a requirement can be envisioned. (1) A chain-growth process in which the formed oligomers preferentially react with monomers, the cyclizable oligomer is thus not skipped (Figure 1a), or (2) the formation of oligomers longer than the cyclizable oligomer is discouraged by steric hindrance involving the "remote" ends of the reacting crescent oligomeric intermediates (Figure 1b).

The two scenarios are first compared by examining results from our work on synthesizing meta-linked crescent oligoamides.[13a] It was observed that coupling monomeric acid chloride **2** with monomeric amine **3** led to dimer **4** in 76% yield after purification (Scheme 2a). Under the same conditions, coupling dimeric acid chloride **5** with dimeric amine **6** led to meta-linked tetramer **7** in the same (76%) yield (Scheme 2b). Thus, the same yield of dimer **4** and tetramer **7** demonstrates that dimers (**5** and **6**) had the same reactivity that associated with monomers (**2** and **3**).

In sharp contrast, coupling tetramers **8** and **9** under the same conditions led to octamer **10** in less than 7% yield (Scheme 2c). The acid chloride group of **8** and the amino group of **9** are placed in local environments very similar to those of dimers **5** and **6**, and are thus unlikely to be deactivated because of their local surroundings. The only difference between products **7** and **10** is that the latter has a length longer than that of one helical turn (~6.5 residues/turn).[12,14] The dramatic difference in the yields of tetramer **7** and octamer **10** thus suggests that a reaction leading to folded oligomers with lengths beyond one helical turn is retarded, which suggests that the efficiency of a coupling reaction is strongly influenced by whether a helical conformation is associated with the product (and thus the corresponding intermediate and transition state). On the basis of the same reasoning, in a macrocyclization reaction, the reaction steps leading to folded oligomeric intermediates with lengths beyond the cyclizable range, i.e., those longer than one helical turn, are hindered.

To further distinguish the two mechanisms, two sets of competition experiments were performed. As shown in Scheme 3a, the reaction between trimeric diamine **11** and diacid chloride **12** should lead to the six-residue macrocycle **1e**. The presence of monomeric diacid chloride **13** would hamper the formation of macrocycle **1e** if, as suggested by the chain-growth process (Figure 1a), diamine **11** reacted with monomer **13** more rapidly than with trimer **12**. Analyzing the crude product from the reaction of **11**, **12**, and **13** (1 equiv each) by MALDI indicated that the major peaks corresponded to that of **1e**, formed from **11** and **12**, and those of other products such an eight-residue macrocycle that could only be formed from the reaction of **11** and **13**.[15] That monomer **13** did not retard the reaction between **11** and **12** was also confirmed by the ^{1}H NMR spectrum of the crude product, which revealed a prominent peak corresponding to **1e**.[15] This result contradicts the chain-growth process mechanism.

Another competition reaction involving dimeric amine **14**, monomeric acid chloride **15**, and dimeric acid chloride **16** was performed (Scheme 3b). The products from this competition experiment should be trimer **17** and tetramer **18** that share the same subunits as those of macrocycles **1**. If the reaction between **14** and **15** were faster than that between **14** and **16**, as suggested by the chain-growth mechanism, trimer **17** would be formed in a faster rate than tetramer **14** and should thus be the dominant product. To compare the yields of **17** and **18**, the reaction mixture, after removing solvent and other volatile components, was directly analyzed by ^{1}H NMR using *p*-xylene as the internal standard.[15] Trimer **17** was found to form in a yield of 37.2% and tetramer **18** was present in 32.1%. The reaction mixture was also separated by column chromatography (silica gel, $CHCl_3$/EtAc/CH_3OH = 6:6:1) into fractions containing trimer **17**, tetramer **18**, and other byproducts. Analyzing the fractions containing **17** and **18**, respectively, by the same ^{1}H NMR method confirmed that the yields of **17** (24.7%) and **18** (23.0%) are similar. Such a result demonstrates that monomer **15** and dimer **16** reacted with dimer **14** in similar rates, which is inconsistent with the chain-growth mechanism.

The above results leave the mechanism shown in Figure 2b as the one that is consistent with the efficient formation of macrocycles **1**. Such a mechanism indicates that in a one-step macrocyclization reaction such as that shown in Scheme 1, steps that lead to oligomers with lengths longer than six-residues are impeded by steric hindrance imposed by the remote ends of the reacting oligomers that fold into rigid, crescent conformations, which in turn favors the generation of the cyclizable, i.e., the immediate oligomeric precursor of a macrocycle.

(13) (a) Yuan, L. H.; Sanford, A. R.; Feng, W.; Zhang, A. M.; Ferguson, J. S.; Yamato, K.; Zhu, J.; Zeng, H. Q.; Gong, B. *J. Org. Chem.* **2005**, *70*, 10660. (b) Zhang, A. M.; Ferguson, J. S.; Yamato, K.; Zheng, C.; Gong, B. *Org. Lett.* **2006**, *8*, 5117.

(14) Gong, B. *Proc. Natl. Acad. Sci. USA* **2002**, *99*, 11583.

(15) Please see Supporting Information.

Scheme 2

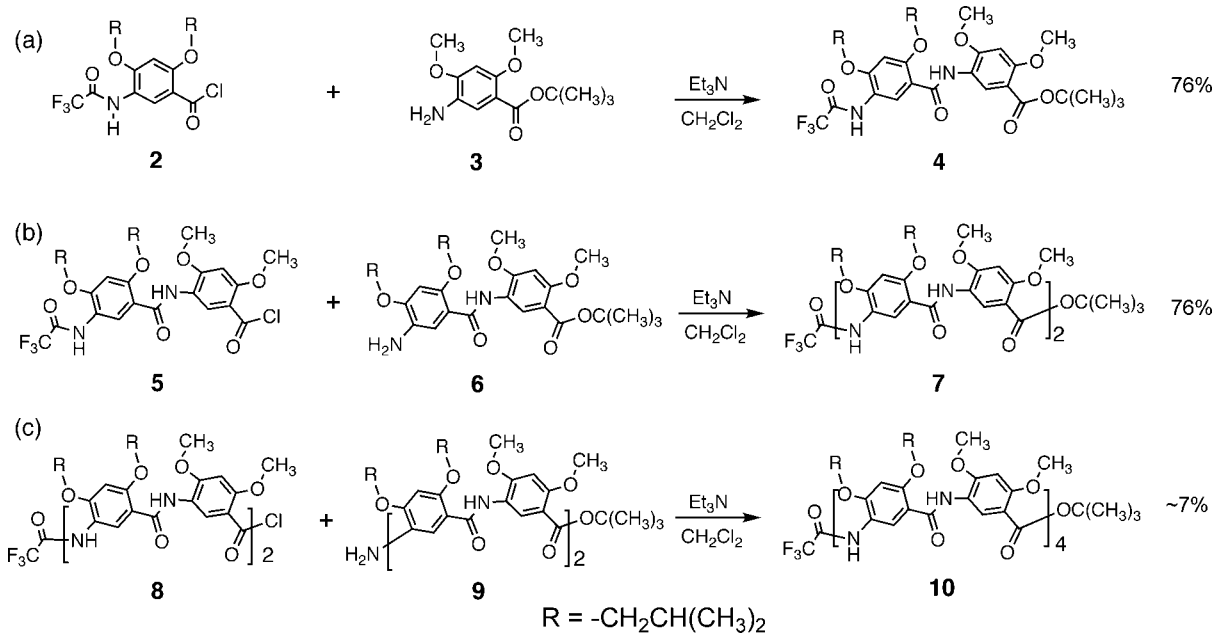

Scheme 3

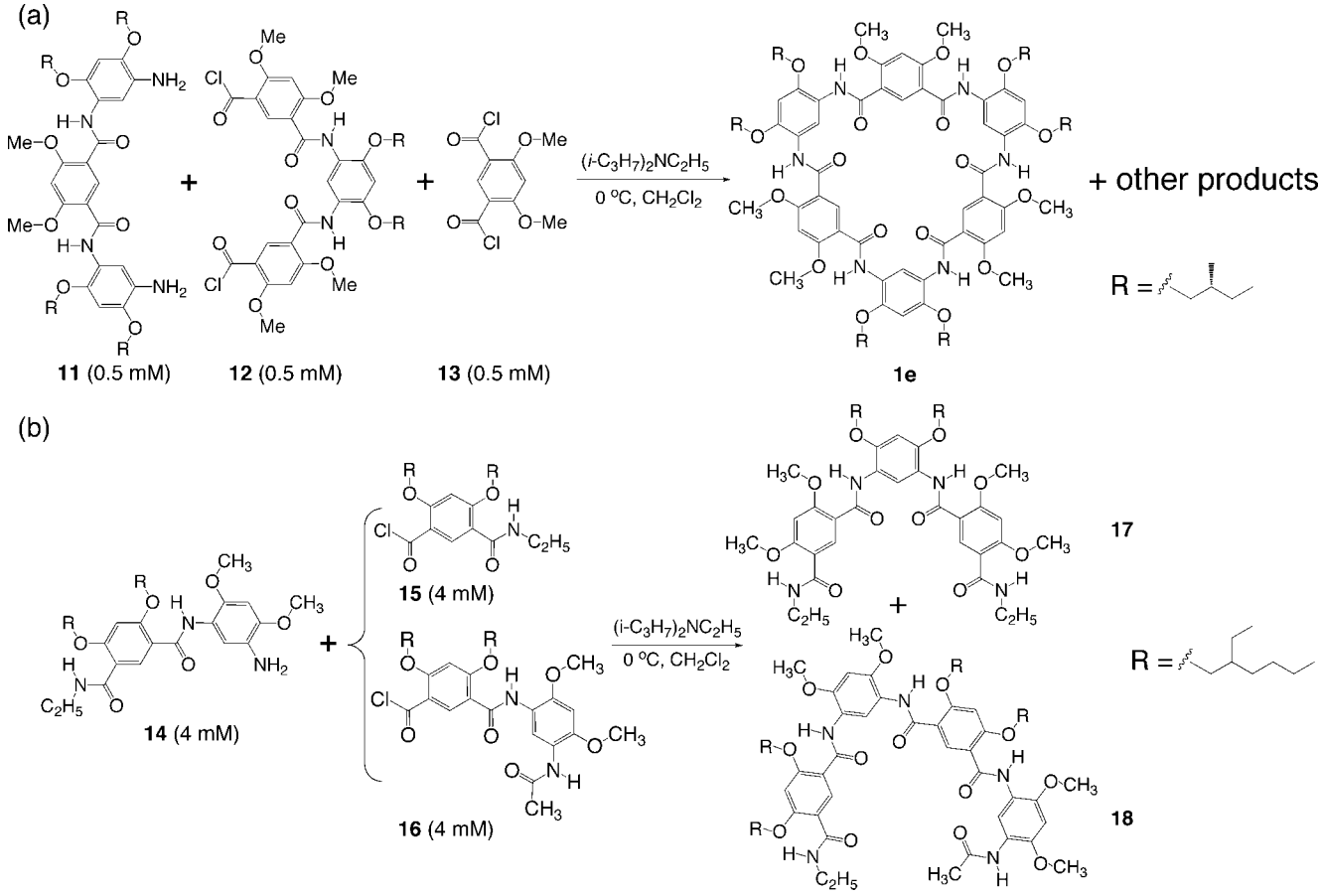

One-Step Preparation of Large Macrocycles. On the basis of the mechanism shown in Figure 1b, other macrocycles involving kinetically controlled bond formation steps should also be formed efficiently as long as their uncyclized oligomeric precursors fold into rigid, crescent conformations. We have demonstrated that aromatic oligoamides consisting of alternating meta- and para-linked benzene units folded into crescent and helical conformations containing large (~30 Å) cavities due to the decreased curvature of their backbones.[14] Can oligoamide macrocycles with meta/para-linked backbones, and thus significantly enlarged lumens, be prepared from the condensation of the corresponding monomers?

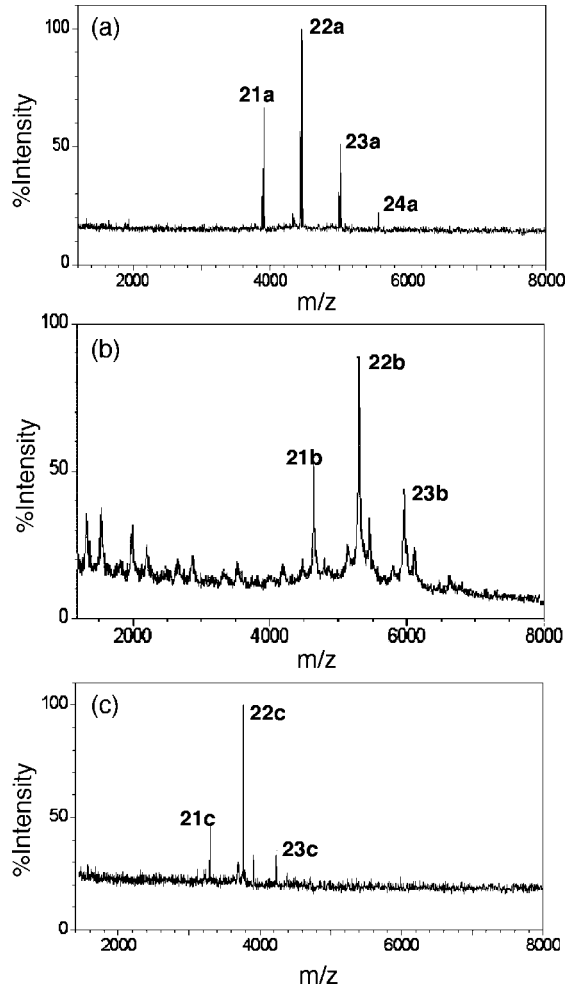

Figure 2. MALDI-TOF spectra of the crude products from the reactions of diacid chloride **19** (1 equiv) with (a) diamine **20a** (1 equiv), (b) diamine **20b** (1 equiv), and (c) diamine **20c** (1 equiv). The peaks for **21a**−**23a** and **21b**−**23b** are from the $[M + Na^+]$ ions. The peaks for **21c**−**23c** are based on the $[M + H^+]$ ions.

To answer this question, diacid chloride **19**, prepared from the corresponding para-diacid by treating with oxalyl chloride, was mixed with meta-diamine **20a** (1 equiv, from the corresponding dinitro compound by hydrogenation) in methylene chloride in the presence of triethylamine at −30 °C (Scheme 4). The reaction mixture was stirred for 4 h, followed by warming up to room temperature and stirring for another 10 h. After being refluxed for 2 h, the reaction mixture was mixed with an excess amount of methanol to precipitate the crude product. The precipitate was collected and washed with methanol, ethyl acetate, and acetone to provide the crude product (84%) as a yellow solid. Examining this crude product using MALDI-TOF revealed the presence of four signals (Figure 2a) corresponding to the 14-residue **21a**, 16-residue **22a**, 18-residue **23a**, and a trace amount of the 20-residue **24a**. Among the three major peaks that correspond to **21a**, **22a**, and **23a**, the signal of 16mer **22a** is the most intense. Repeated recrystallization from CH_2Cl_2/MeOH and DMF/acetone provided the product as a yellow solid (81%).

Treating **19** with diamines **20b** and **20c**, respectively, led to similar results. As revealed by MALDI-TOF, the 14-, 16-, and 18-residue macrocycles **21b**, **22b**, and **23b** (Figure 2b), and **21c**, **22c**, and **23c** (Figure 2c), were obtained from these one-step condensation reactions. An overall yield of about 70% was observed in each case after repeated recrystallization from CH_2Cl_2/MeOH and CH_2Cl_2/EtOAc (**21b**, **22b**, and **23b**) or DMF/acetone (**21c**, **22c**, and **23c**). Similar to **22a**, the signals of the 16-residue **22b** and **22c** are the most intense in the MALDI spectra of the crude products from both reactions. In contrast to the presence of a very weak signal for 20mer **24a** (Figure 2a), the corresponding 20-residue **24b** and **24c** were not detected from the crude products of the corresponding reactions. These results demonstrate that, similar to six-residue **1**, the efficient formation of the much larger macrocycles **21**−**23** is determined by the shape-persistent, crescent oligoamide backbones of their immediate oligomeric precursors while being independent of the type of side chains.

That three, instead of one, macrocycles were obtained from the above one-step reactions can be attributed to the small variability associated with the bond angles of the amide linkages that are rigidified by three-center H-bonds. The variability associated with amide bond angles was revealed by examining the single-crystal structures of crescent aromatic oligoamides that share the same H-bond-rigidified secondary amide groups as those in the backbones of the macrocycles. On the basis of

Scheme 4

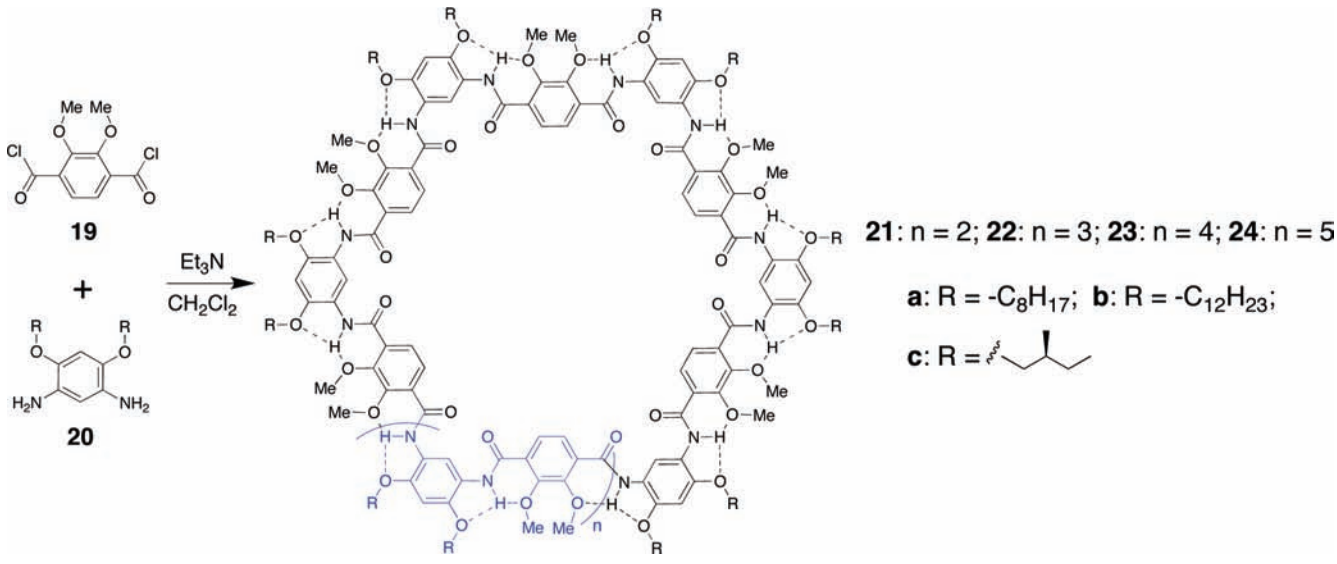

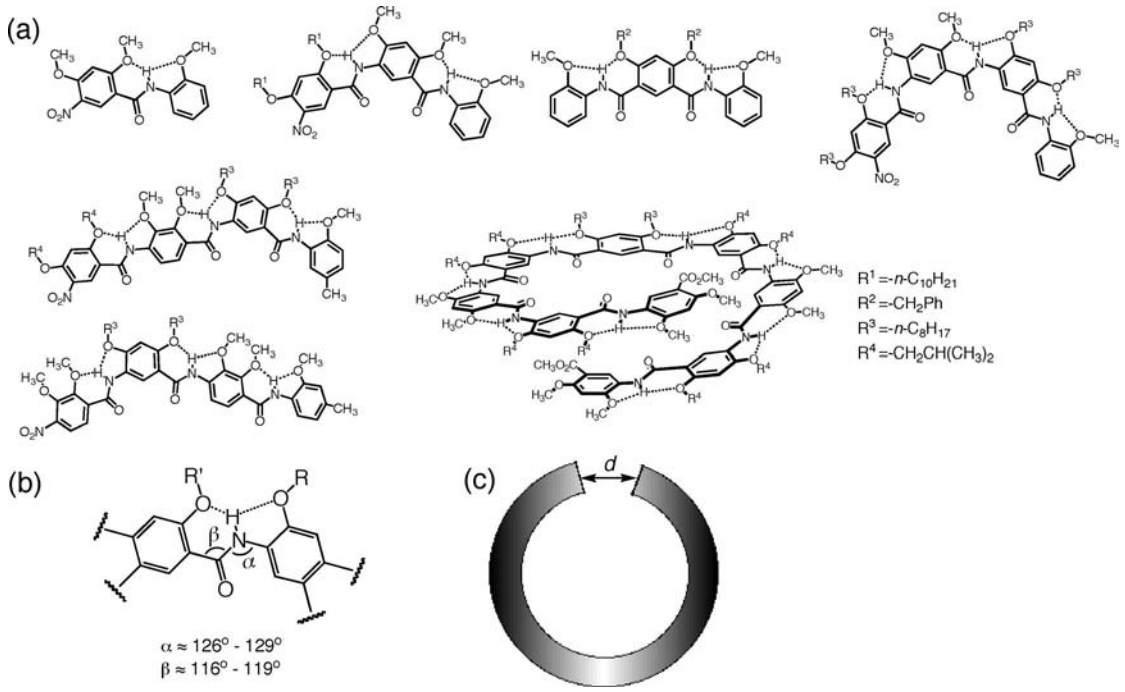

Figure 3. (a) Examining the known crystal structures of crescent oligoamides reveals (b) the values of amide bond angles α and β vary within narrow ranges. (c) The small variability contributed by each bond angle allows the end-to-end distance d of an uncyclized crescent oligoamide to fluctuate. Compared to that consisting of meta-linked benzene residues, an oligomer consisting alternating meta- and para-linked is less curved and thus need to reach a longer length, i.e., involving a larger number of residues or amide linkages, before its two ends can reach a reacting distance. The combined variability of the numerous amide bond angles allows several, instead of one, uncyclized meta/para-linked oligomers with lengths within a narrow range to place their two reacting ends in a distance within which cyclization could happen.

the crystal structures of a dimer, two trimers, two tetramer, and a nonamer (Figure 3a), which were reported by us before,[12,14] bond angle α is found to vary from about 126° to 129°, while β fluctuates from 116° to 119° (Figure 3b). Compared to the six-residue precursors of macrocycles **1**, the immediate precursor of any one of the meta/para-linked macrocycles is much longer, containing a larger number of residues and amide linkages. While such a meta/para-linked oligomeric precursor is now well documented to adopt a crescent, tape-like backbone that is enforced by the three-center H-bonds, the combined (added) variability of the numerous amide bond angles leads to additional flexibility in the overall curvature of the oligoamide backbone. Therefore, the fluctuation of the overall curvature of the uncyclized precursors leads to the variation of their end-to-end distance d (Figure 3c), which means that several, i.e., three in this case, uncyclized oligomers with lengths within a narrow range can have their two ends to reach a reacting distance, leading to more than one cyclized product.

Although results from the MALDI-TOF experiments provided diagnostic evidence for the generation of the macrocycles, the yields of **21c**, **22c**, and **23c** were quantified by separating these oligomers from the crude product using column chromatography (silica gel, $CHCl_3$/EtOAc/CH_3OH = 10:1:0.2−10:1:0.5, v/v). The yields were 24% (**21c**), 37% (**22c**), and 9% (**23c**) after separation, which confirmed that the relative ratio of the three macrocycles revealed by MALDI was reliable. Similar to those observed for the six-residue macrocycles **1**, these yields deviate dramatically from results obtained from kinetic simulation. On the basis of a typical polycondensation reaction in which all the reactive species, i.e., monomers and oligomers, have the same reactivity, kinetic simulation shows that the immediate oligomeric precursors leading to macrocycles **21**, **22**, and **23** should be formed in an overall maximum yield of 43% (16% for **21**, 15% for **22**, and 12% for **23**).[15] These results are consistent with the above mechanism involving remote steric effects brought about by the folded conformations of the transition states and reaction intermediates of the macrocycles.

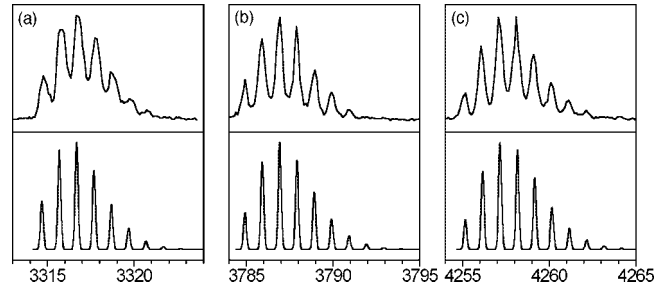

Figure 4. Isotope distribution patterns of the [M + Na^+] peaks of (a) **21c**, (b) **22c**, and (c) **23c**. (top, experimental; bottom, calculated).

The separated macrocycles were characterized by MALDI-TOF, ^{1}H, and ^{13}C NMR.[15] The identities of macrocycles **21c**−**23c** were shown by matching the isotope distributions of their [M + Na^+] peaks with computer simulated results (Figure 4). The cyclic structures of **21c**−**23c** were also supported by the simplicity of their ^{1}H NMR spectra.[15] The ^{1}H NMR spectrum of each macrocycle contains four ^{1}H signals in the region ranging from 6.4 to 10.6 ppm, corresponding to one group of equivalent amide and three groups of equivalent aromatic protons that belong to the two types of monomeric residues in each of the macrocycles (Figure 5). Consistent with the symmetrical nature of the corresponding cyclic structures, the ^{13}C NMR spectra of these compounds exhibit similar simplicity.[15]

Exclusive Formation of the 16- and 18-Residue Macrocycles. The one-step condensation of monomeric **19** and **20** has provided an efficient method for preparing a new series of large

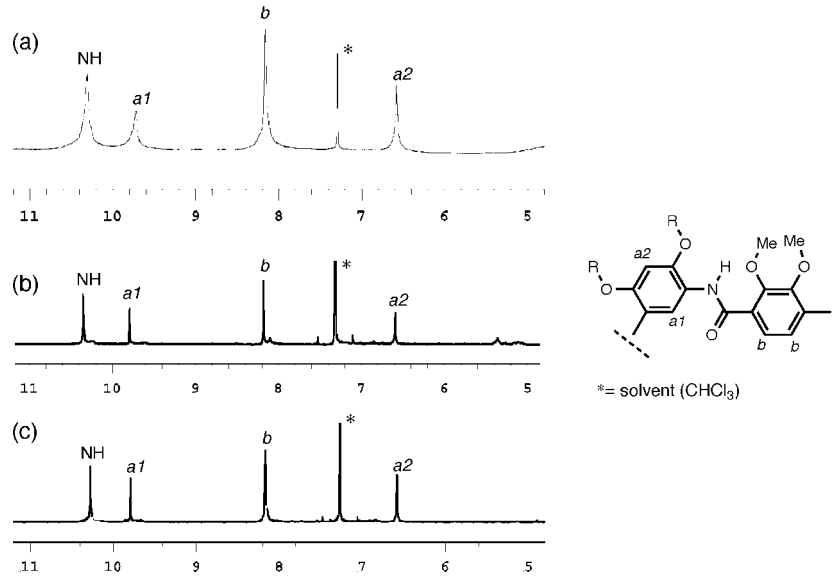

Figure 5. ^{1}H NMR signals of the aromatic and amide region of (a) **21c**, (b) **22c**, and (c) **23c**.

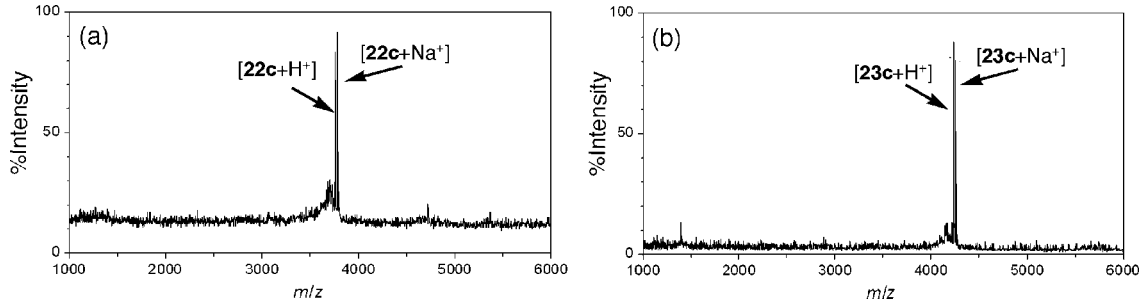

Figure 6. MALDI-TOF spectra of the crude products from the condensation of diacid chloride **19** with (a) trimer diamine **25**, and (b) pentamer diamine **26**.

aromatic oligoamide macrocycles having persistent shapes and noncollapsible cavities. For applications that do not require a uniform cavity, such as the preparation of bulk nanoporous materials, mixtures containing the three macrocycles may suffice. However, in many other cases, a single product is required. On the basis of the one-step condensation reaction involving **19** and **20**, tedious separation of the products using column chromatography has to be performed if a specific macrocycle is the desired target.

To circumvent this limitation, an alternative strategy allowing the selective formation of a single macrocyclic product was designed. As shown in Scheme 4a, instead of performing the condensation reaction using only monomeric reactants, trimeric diamine **25**[15] was treated with diacid chloride **19**. In this case, depending on the number of reacting components involved in the reaction, macrocycles with 4, 8, 12, 16, 20, or more monomeric residues could *in theory* be formed, among which only the 16-residue **22c** belongs to the "allowable" group of the three products detected in the condensation of monomers **19** and **20**. Thus, the 16-residue **22c** should appear as the dominant product from the condensation between trimer **25** and diacid chloride **19**, while the 14-residue **21c** and 18-residue **22c**, which appeared in the condensation between **19** and **20**, could not be obtained from any combination of **25** and **19**. Such an expectation was confirmed by MALDI-TOF (Figure 6a), which revealed a nearly exclusive formation of **22c** from the reaction of **25** and **19**. Macrocycle **22c** was obtained in a yield of 83% after precipitation and washing with methanol. Purification by flash column chromatography (silica gel, $CHCl_3$/EtOAc/methanol (10:1:0.2−10:1:0.5 v/v)) led to the isolation of pure **22c** in a yield of 70%.

The effectiveness and generality of this strategy were demonstrated again by coupling pentameric diamine **26**[15] with diacid chloride **19** (Scheme 5b). The combination of **26** with diacid chloride **19** could lead to macrocycles containing 6, 12, 18, 24, or more monomeric residues, among which only the 18-residue **23c** belong to the group of the three macrocycles detected from the one-step condensation of monomers. As shown in Figure 6b, MALDI-TOF revealed the formation of the 18-residue **23c**, which appeared as the only major product from the reaction between **19** and **26**. The essentially pure **23c** was obtained in 85% upon precipitating and washing with methanol. Thus, a target macrocycle can be selectively obtained from the condensation of simple oligomeric diamines and acid chloride **19**. Such a strategy obviates the formation of other undesired products.

Ab initio calculation. The structures of macrocycles **21**, **22**, and **23** (R replaced with methyl) were optimized by using an ab initio method at the B3LYP/6-31(g)d level of theory. As shown in Figure 7, these macrocycles have backbones rigidified by three-center H-bonds, with large, well-defined internal cavities of ∼2.2, 2.5, and 2.9 nm across. The 14-residue **21** has a conformation resembling a shallow bowl, while the 16-residue **22** has a flat backbone and the overall shape of the 18-residue **23** is also flat with a slightly twisted backbone. These results indicate that, among the three macrocycles, the 16-residue **22**

Scheme 5

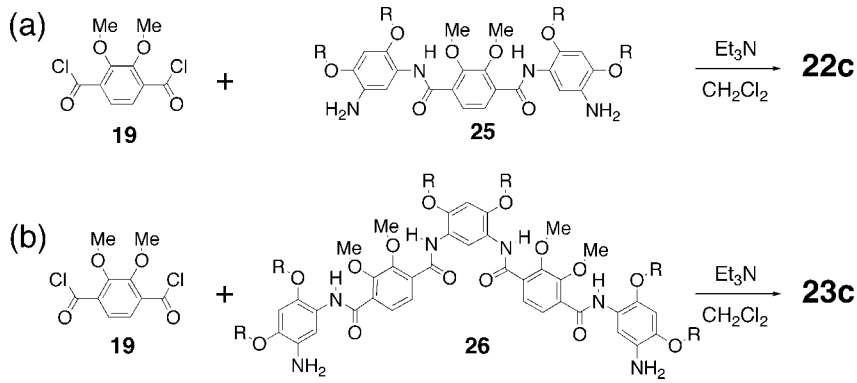

has the smallest ring strain which leads to a backbone that is least twisted and thus most befits three-center H-bonding, while the 14-residue **21** and 18-residue **23** have backbones that deviate slightly from planarity, possibly due to small ring strain. These very large macrocycles, along with the much smaller the six-residue ones we discovered before, represent a new class of readily available macrocyclic molecules having persistent shapes with noncollapsible, hydrophilic internal cavities.

Conclusions

By comparing the formation of crescent oligoamides of different lengths, and by carrying out competition reactions involving monomeric and oligomeric reactants, one out of two possible mechanisms, involving a remote steric effect that inversely influences coupling reactivity, was able to account for the preferred formation of the immediate precursors of macrocycles **1**, which also explains the dearth of other longer (overshooting) oligomers with lengths beyond the cyclizable range. Consistent with such a mechanism, the formation of much larger aromatic oligoamide macrocycles showed the same high efficiency based on multicomponent condensation reactions between the corresponding diamines and diacid chloride **19**, which resulted in macrocycles consisting of alternating meta- and para-linked residues. The resultant shape-persistent oligoamide macrocycles are very large and have large, noncollapsible lumens. The condensation of monomeric diamines with diacid chloride **19** led to macrocyclic products with a narrow product distribution and high overall yields. An alternative strategy based on the condensation between a trimeric or a pentameric diamine and diacid chloride **19** led to a nearly exclusive formation of the 16- and 18-residue macrocycles. The ready availability of these novel macrocycles makes it possible to further probe their unique properties and potential applications. For example, the large aromatic surfaces associated with these macrocycles could result in very strong intermolecular stacking interactions, which may lead to robust self-assembling structures. Strategies for aligning these macrocycles could lead to nanotubes containing large hydrophilic pores. With their nanosized, hydrophilic lumens, these macrocycles could serve as hosts for large hydrophilic guests. With their readily modifiable side chains, macrocycles compatible to different media can be conveniently designed. Given the large numbers of components, i.e., 14, 16, and 18 monomeric units, involved in these marocyclization reactions, the high overall yields and narrow product distribution are phenomenal, which contrast sharply with the low yields of target products observed in other kinetic macrocyclic condensation reactions. Systematic studies are being pursued to reveal the details of the mechanism behind these highly efficient, kinetically controlled macrocyclization reactions. Results and insights from this and ongoing studies should guide the efficient synthesis of shape-persistent macrocycles based on other folded oligomeric precursors with rigidified, folded backbones.[16]

Experimental Procedures

All chemicals were purchased from Aldrich or Fisher (Acros) and were used as received unless otherwise indicated. NMR analyses were carried out on Varian INOVA 500 spectrometer. Tetramethylsilane (TMS) was used as the internal standard for ^{1}H and ^{13}C NMR. Chemical shifts are reported in ppm values downfield from tetramethylsilane and *J* values are reported in Hz. MALDI-TOF MS spectra were recorded on a Bruker Bifrex IV MS spectrometer using 2,5-dihydroxybenzoic acid (DHB) or dithranol (DTH) as the matrices.

General Synthetic Procedures. Diamine **20**,[13,15] prepared from the corresponding dinitro compound (1.18 mmol) by catalytic

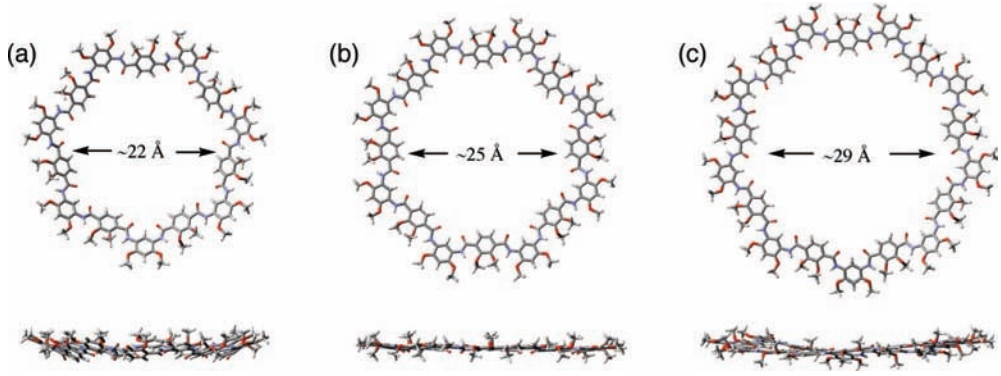

Figure 7. Top and side views of the structures of macrocycles (a) **21**, (b) **22**, and (c) **23** optimized at the B3LYP/6-31(g)d level. For simplicity, all side chains are replaced with methyl groups.

hydrogenation, and acid chloride **19**,[13,15] prepared from the corresponding diacid (1.18 mmol) and oxalyl chloride (446 mg, 3.54 mmol) in CH_2Cl_2 with 1−2 drops of DMF, were stirred in CH_2Cl_2 (10 mL) at −20 °C for 4 h, and then at room temperature for 10 h in the presence of triethylamine (358 mg, 3.54 mmol). The reaction mixture was stirred at reflux for 2 h, to which methanol (100 mL) was added to cause precipitation. The solid was collected, washed with MeOH, acetone, ethyl acetate to provide the crude product which was further purified by repeated recrystallization from CH_2Cl_2/MeOH and CH_2Cl_2/acetone or DMF/acetone. As indicated by MALDI-TOF, the crude and further purified products from all three sets of reactions between acid chloride **19** and diamines **20** contained the 14-, 16-, and 18-residue macrocycles **21**, **22**, and **23** as the dominant species, with the signal corresponding to 16-residue **21a**, **22b**, or **23c** being the strongest in each case.

Macrocycles 21a, 22a, and 23a. The crude product (550 mg, 84%) was obtained as yellow solid. MALDI-TOF indicated the presence of four signals, consisting of cyclic 14mer, 16mer, 18mer, and 20mer. Among them, the 16-residue **22a** showed the most intense signal. Repeated recrystallization from CH_2Cl_2/MeOH and DMF/acetone provided the product as yellow solid (530 mg, 81%). The product is slightly soluble in chloroform and methylene chloride.

Macrocycles 21b, 22b, and 23b. The crude product (667 mg, 84.7%) was obtained as a yellow solid. MALDI-TOF indicated the presence of three signals, corresponding to the three macrocycles **21b**, **22b**, and **23b**. Repeated recrystallization from CH_2Cl_2/MeOH provided the product as a yellow solid (549 mg, 69.8%). The product mixture was soluble in chloroform and methylene chloride.

Macrocycles 21c, 22c, and 23c. The crude product (483 mg, 87%) was obtained as a yellow solid. MALDI-TOF indicated the presence of three signals, corresponding to the three macrocycles **21c**, **22c**, and **23c**. Repeated recrystallization from CH_2Cl_2/MeOH and DMF/acetone provided the product as a yellow solid (389 mg, 70.1%). The product mixture was slightly soluble in chloroform and methylene chloride and soluble in a mixed solvent of chloroform and methanol.

Separation of 21c, 22c, and 23c by Column Chromatography. The crude product (100 mg) was subjected to purification by chromatography (silica gel, $CHCl_3$/EtOAc/MeOH, 10:1:0.2 first and then 10:1:0.5 v/v). The separated macrocycles **21c**, **22c**, and **23c** were then characterized by MALDI-TOF, ^{1}H, and ^{13}C NMR.

Macrocyle 21c. Yield after isolation: 24%.^{1}H NMR (500 MHz, $CDCl_3$) δ 10.23 (s, 14H), 9.64 (s, 7H), 8.12 (s, 14H), 6.57 (s, 7H), 4.05 (s, 42H), 3.94 (m, 14H), 3.88 (m, 14H), 1.98 (m, 14H), 1.70 (m, 14H), 1.36 (m, 14H), 1.11 (d, J = 6.5 Hz, 42H), 1.00 (t, J = 7.5 Hz, 42H). ^{13}C NMR (75.5 MHz, $CDCl_3$) δ 161.4, 151.4, 145.6, 130.7, 127.0, 120.8, 96.9, 74.0, 61.9, 35.0, 26.1, 16.5, 11.4; MALDI-TOF m/z, Calcd for $C_{182}H_{238}N_{14}O_{42}$ 3291.69 (M^+), found 3314.7 ($M + Na^+$).

Macrocycle 22c. Yield after isolation: 37.0%. ^{1}H NMR (500 MHz, 98%$CDCl_3$/2%CD_3OD) δ10.34 (s, 16H), 9.78 (s, 8H), 8.17 (s, 16H), 6.58 (s, 8H), 4.08 (s, 48H), 3.96 (m, 16H), 3.90 (m, 16H), 1.99 (m, 16H), 1.73 (m, 16H), 1.36 (m, 16H), 1.14 (d, J = 6.5 Hz, 48H), 1.03 (t, J = 7.0 Hz, 48H). ^{13}C NMR (75.5 MHz, 98%$CDCl_3$/2%CD_3OD) δ 161.4, 151.4, 145.7, 130.8, 127.1, 120.9, 97.0, 74.0, 61.9, 35.1, 26.1, 16.5, 11.4; MALDI-TOF m/z, Calcd for $C_{208}H_{272}N_{16}O_{48}$ 3784.92 ($M + Na^+$), found 3784.6 ($M + Na^+$).

Macrocycle 23c. Yield after isolation: 9.2%. ^{1}H NMR (500 MHz, $CDCl_3$) δ 10.27 (s, 18H), 9.78 (s, 9H), 8.16 (s, 18H), 6.57 (s, 9H), 4.05 (s, 54H), 3.94 (m, 18H), 3.88 (m, 18H), 1.99 (m, 18H), 1.72 (m, 18H), 1.37 (m, 18H), 1.12 (d, J = 6.5 Hz, 54H), 1.01 (t, J = 7.5 Hz, 54H). ^{13}C NMR (3% CD_3OD/$CDCl_3$) δ 11.16, 16.25, 25.90, 34.87, 61.79, 63.30, 73.85, 96.73, 120.27, 126.66, 130.49, 145.74, 151.41, 161.48. MALDI-TOF m/z, Calcd for $C_{234}H_{306}N_{18}O_{54}$ 4232.18 (M^+), found 4233.1 ($M + H^+$).

Exclusive Formation of Macrocycle 22c. Acid chloride **19**, prepared from the corresponding diacid (75 mg, 0.33 mmol) by treating with oxalyl chloride in CH_2Cl_2 in the presence of ∼1 drop of DMF,[15] was dissolved in methylene chloride (40 mL). A solution of trimer diamine **25**, prepared from the corresponding dinitro trimer (377 mg, 0.33 mmol) by catalytic hydrogenation,[15] in methylene chloride (40 mL) containing triethylamine (134 mg, 1.32 mmol) were added dropwise to the solution of acid chloride **1p**. The reaction mixture was stirred at −20 °C for 4 h, and then at room temperature for 8 h, after which was heated at reflux for 2 h. Methanol was added to cause precipitation and the solid was collected, washed with MeOH, acetone, and ethyl acetate to provide 337 mg of yellow solid. The crude product was obtained in a yield of 83.3%. Flash chromatography ((silica gel, $CHCl_3$/EtOAc/MeOH (10:1:0.2 first, then 10:1:0.5 v/v) provided macrocycle **22c** as a yellow solid in 69.6%. The MALDI, ^{1}H, and ^{13}C NMR spectra are the same as those of **22c** isolated by column chromatography.

Exclusive Formation of Macrocycle 23c. Pentamer diamine **26**, prepared from the corresponding dinitro pentamer (250 mg, 0.20 mmol) by catalytic hydrogenation,[15] was mixed with acid chloride **19** (1 equiv) in CH_2Cl_2 (30 mL) in the presence of triethylamine at −20 °C. The mixture was stirred at this temperature for 4 h, and then at room temperature for 8 h, after which was heated at reflux for 2 h. The reaction mixture was isolated by precipitation with methanol. The precipitate was washed with methanol, ethyl acetate, and acetone, affording the crude product as a yellow solid (236 mg, 84%), which MALDI showed to be essentially pure macrocycle **23c**. The MALDI, ^{1}H, and ^{13}C NMR spectra are the same as those of the **23c** isolated by column chromatography.

Ab initio computations. Ab initio density-functional theory (DFT) computation was carried out using the Gaussian 03 package.[17] The geometry of **21**−**23** was optimized by using the B3LYP/6-31G(d) level of theory and basis set. DFT computations show that **21** has shape similar to a shallow bowl, whereas **22** is a planar ring and **23** is slightly twisted with a small out-of-plane angle.

Acknowledgment. This work was supported by the National Natural Science Foundation of China (No. 20672078 to LHY), the National Science Foundation of the U.S.A. (CHE-0314577 and CHE-0701540 to B.G. and X.C.Z.), the Nebraska Research Initiative (to X.C.Z.) for support of this research, and by the Research Computing Facility at University of Nebraska−Lincoln and Holland Computing Center at University of Nebraska−Omaha.

Supporting Information Available: Results from the competition reactions, procedures for synthesizing trimer **25** and pentamer **26**, analytical data, additional MS and NMR spectra, results of kinetic simulation, and complete refs 14 and 17. This material is available free of charge via the Internet at http://pubs.acs.org.

JA807935Y

(16) (a) Gong, B. *Acc. Chem. Res.* **2008**, *41*, 1376. (b) Li, Z.-T.; Hou, J.-L.; Li, C.; Yi, H.-P *Chem. Asian J.* **2006**, *1*, 766. (c) Huc, I. *Eur. J. Org. Chem.* **2004**, 17.

(17) Frisch M. J.; *Gaussian03, Revision C.02*; Gaussian, Inc.: Pittsburgh, 2003.